

Geometric and electronic structures of graphitic-like and tubular silicon carbides: *Ab-initio* studies

Ming Yu, C. S. Jayanthi, and S. Y. Wu

Department of Physics, University of Louisville, Louisville, Kentucky 40292, USA

(Received 19 May 2010; published 6 August 2010)

The optimized structures of graphitic-like sheets (i.e., single and multilayered) as well as tubular structures (i.e., both single-wall and double-wall) of SiC including their electronic structures are investigated using *ab-initio* simulations within the framework of the density-functional theory. We find that: (i) SiC graphitic-like structures form sp^2 -like bonding, although the bulk phases of SiC exhibit sp^3 bonding, (ii) the interplanar spacing in a multilayer graphitic sheet depends on how the atoms are arranged in adjacent SiC bilayers (e.g., Si-C or C-C interplanar order). It is smaller for the Si-C ordering (~ 3.7 Å) than for the C-C ordering (~ 4.5 Å). Our analysis indicates that the electrostatic interaction between the bilayers is responsible for the smaller interplanar spacing exhibited by the Si-C ordering. These findings provide the basis for the interpretation of experimental observations that display two different values for intershell distances (~ 3.8 Å or ~ 4.8 Å) in SiC-based multiwall nanotubes.

DOI: [10.1103/PhysRevB.82.075407](https://doi.org/10.1103/PhysRevB.82.075407)

PACS number(s): 61.46.Fg, 68.65.Ac

I. INTRODUCTION

Recent research interest in silicon carbide based nanostructures is prompted by the experiments on the synthesis of SiC nanotubes and nanowires.¹⁻⁴ It is well known that bulk SiC exhibits robust electrical, thermal, and mechanical properties with wide-ranging applications in the semiconductor industry.⁵ Therefore, it is of interest to understand how these properties would get altered in reduced dimensions. Furthermore, bulk silicon carbide manifests in many polymorphic forms due to different stacking arrangements of SiC bilayers along the *c*-axis of cubic zinc-blende (β -SiC) and along the $\langle 0001 \rangle$ direction of the hexagonal wurtzite structure (α -SiC). It is, therefore, natural to ask the question: “how such polymorphism will manifest itself in quasi-one-dimensional and two-dimensional structures of SiC?” We, therefore, will investigate in this work the structural stability of graphitic-like and multi-layer SiC structures, as well as single-wall and double-wall SiC nanotubes from energetic considerations, stacking arrangements, etc. Their optimized geometric structures and band structures will be investigated using *ab-initio* studies based on the density-functional theory (DFT). These studies will allow us to understand how the bulk electronic properties⁵ (in particular, energy gaps) will be modified by the reduced dimensionality of nanostructures, and, thus, providing an assessment of the devices to be fabricated with SiC nanostructures.

Several experimental groups have successfully synthesized quasi-one-dimensional SiC-based structures.¹⁻⁴ These quasi-one-dimensional SiC structures include SiC nanowires (NWs),¹⁻³ SiC nanotubes (NTs),⁴ and SiC multiwalled nanotubes (MWNTs).¹ TEM images of β -SiC (Refs. 1 and 2) NWs oriented along $\langle 111 \rangle$ reveal an interlayer spacing of 2.5 Å. The same spacing is also found in the synthesized β -SiC NTs.⁴ On the other hand, HRTEM images of synthesized multiwalled SiC nanotubes¹ (produced by disproportionate reaction of SiO with multiwalled carbon nanotubes) reveal intershell separations both at 3.8 Å and around 4.2–4.5 Å.

The above observations raise the following questions: (i) does the large intershell spacing in SiC MWNTs imply the existence of graphitic-like SiC structures, (ii) if, indeed, a stable SiC sheet can be formed, will it have sp^2 -like or sp^3 -like bonding, (iii) what is the reason for the manifestation of different values of the intershell spacing in SiC MWNTs, and (iv) do the interlayer stacking of atoms dictate the interlayer (or intershell) spacing in multi-layer sheets (or multiwall SiC NTs)? A recent DFT-based study of SiC NTs has found a weakly buckled structure in SiC NTs when their diameters are less than 1.6 nm.⁶ This implies a weak ‘ sp^3 -like’ bonding in these SiC NTs. The bonding nature of Si-C bond in the SiC graphitic-like structure, however, is still unclear. It is therefore important to ascertain various possible aspects of the bonding nature of the Si-C bond for a comprehensive understanding of the structural and other properties of SiC based systems.

In the present work, we have undertaken a computational study that investigates the structure, stability, and bonding characteristics of single-layer and multilayered SiC sheets in order to clarify the bonding nature in SiC graphitic-like structures and to provide an answer to the experimental observations of several possible intershell separations in SiC MWNTs. Structural relaxations are performed using DFT-based simulations as implemented in the Vienna *ab-initio* simulation package (VASP).⁷ Additionally, a local analysis technique as developed in Ref. 8 and a semiempirical Hamiltonian as developed in Ref. 9 will be used for the analysis of bonding characteristics. Section II is devoted to the structural and bonding properties of SiC sheets starting from various buckled initial configurations. Crudely speaking, if the SiC graphitic sheet relaxes to a buckled structure, then that is indicative of a sp^3 -like bonding, while a flat relaxed SiC sheet is indicative of a sp^2 -like bonding. The bond-charge analysis technique⁸ will provide a more quantitative analysis of the bonding nature. Section III focuses on the energetics of single-wall SiC nanotubes of various diameters. For each diameter, total energies SiC SWNTs are calculated relative to the SiC graphitic sheet for two types of initial configurations:

(i) buckled SiC NTs and (ii) un-buckled SiC NTs. Section IV focuses on structural optimizations of multi-layered SiC sheets with two, three, and four bilayers of SiC, and these studies elucidate the connection between bilayer stacking arrangements and the interlayer spacing. In Sec. V, a further confirmation on the correlation between the stacking arrangement of SiC bilayers and the inter-shell distance is offered through studies on the energetics of SiC DWNTs. Section VI summarizes our results and conclusions.

II. SiC GRAPHITIC-LIKE SHEETS

A. Structural optimizations of SiC graphitic-like sheets

This section focuses on the study of the structural optimization of SiC graphitic-like structures based on *ab-initio* simulations as implemented in the VASP.⁷ The calculations were performed within DFT/GGA using plane-wave basis sets, ultrasoft pseudopotentials (U.S.-PP),¹⁰ and the Perdew and Wang (PW '91) exchange correlations.¹¹ We employed the two-dimensional periodic boundary condition in the layered plane with a vacuum region (15 Å) between sheets to ensure that there was no interaction between the SiC graphitic-like layers. The cutoff energy for the plane wave basis set was 456 eV, and several sets of k points (i.e., 26, 52, 186, and 512 k points) based on the Monkhorst-Pack scheme¹² were considered for the convergence of the total energy. The energy convergence for the self-consistent calculation was set to 10^{-5} eV, and the structure was relaxed using the conjugate-gradient (CG) algorithm until the atomic forces were less than 10^{-3} eV/Å.

In our study of the structural optimization of SiC graphitic sheets, we intentionally started with initial configurations that were buckled. Since bulk SiC has tetrahedral symmetry, sp^3 -type bonding may be a possible bonding in the SiC graphitic structure too. We considered different buckling angles $\theta = \sin^{-1}(z_{\text{buckled}}/b)$ (where z_{buckled} is the vertical separation between Si and C atoms in the bilayer, and b , the bond length of SiC) (see Fig. 1(b)). We varied z_{buckled} between the values 0.1–0.63 Å. The relaxed final configuration corresponding to all of these initial configurations is a regular flat graphitic-like form with buckling less than 1.0×10^{-3} Å (see the right panel of Fig. 1). The optimized Si-C bond length is 1.78 Å (*viz.* 1.89 Å in bulk SiC). The cohesive energy per atom of the optimized SiC graphitic sheet is 0.49 eV higher than that

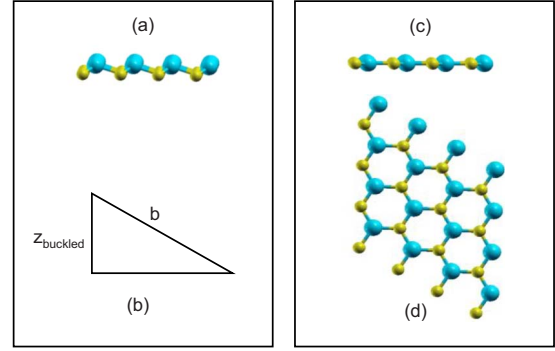


FIG. 1. (Color online) (a) A buckled initial configuration of the relaxed SiC graphitic-like sheet (yellow: carbon atoms; blue: silicon atoms). (b) Quantities defining the buckling angle (see the text). (c) The side view of the relaxed SiC sheet. (d) The top view of the relaxed SiC sheet. Several initial configurations were considered in the calculations with z_{buckled} ranging from 0.1 to 0.63 Å. Regardless of the buckling angle considered for the initial configuration, the final relaxed structure was always a nearly flat sheet with $b = 1.78$ Å and $z_{\text{buckled}} = 0.0007$ Å, as shown in (c).

of bulk β -SiC. This energy difference is similar to that found in graphitic-like structures of group-III nitrides,^{13–15} suggesting the possibility of the formation of SiC graphitic-like sheet as a metastable or intermediate state under appropriate conditions.

B. Analysis of the bonding nature in graphitic-like sheets

While the existence of the stable *flat* SiC graphitic-like structure already suggests that Si and C atoms may form sp^2 -type bonding, an understanding of the underlying reason for the transition of the “unstable” buckled graphitic-like SiC structure to a “stable” flat graphitic-like sheet would shed more light on this scenario. For this purpose, we performed an analysis of the local bond charge and bond energy⁸ based on the self-consistent and environment-dependent (SCED) Hamiltonian^{9,16,17} developed in the framework of linear combination of atomic orbitals (LCAO). Successful applications of the SCED-LCAO Hamiltonian to SiC nanostructures can be found in Ref. 17.

Table I shows the results of our calculation based on the SCED-LCAO Hamiltonian^{9,17} for the orbital bond charge be-

TABLE I. Results of the local analysis for the bulk (zinc-blende) and graphitic-like SiC structures (buckled and flattened) that include the orbital bond charges ($N_{ij}(\alpha)$, $\alpha = \sigma, \pi$), the ratio of the π -orbital bond charge to the σ -orbital bond charge ($N_{ij}(\pi)/N_{ij}(\sigma)$), the bonding energy ($-E_{ij}$), and the charge (N_i) at site i .

Structure	$N_{ij}(\sigma)$	$N_{ij}(\pi)$	$N_{ij}(\pi)/N_{ij}(\sigma)$	E_{ij} (eV)	N_i
Zinc-blende	0.29 e	0.00 e	0.00	-7.41	4.31 (C) 3.69 (Si)
Initial (buckled) graphitic-like sheet	0.31 e	0.02 e	0.05	-8.07	4.19 (C) 3.81 (Si)
Relaxed (flattened) graphitic-like sheet	0.32 e	0.10 e	0.30	-10.42	4.32 (C) 3.68 (Si)

tween atomic sites i and j ($N_{ij}(\alpha)$, $\alpha = \sigma, \pi$), the ratio of the π orbital bond charge to the σ orbital bond charge ($N_{ij}(\pi)/N_{ij}(\sigma)$), the bonding energy ($-E_{ij}$) between atomic sites i and j , and the charge on the atomic site i (N_i) for the bulk SiC (zinc blende) and graphitic-like SiC sheet (buckled and flattened), respectively (see, Ref. 8 for the definition of the above quantities). It can be seen that in the case of bulk β -SiC the bond charge is distributed only on the σ orbital with no charge distribution on the π orbital, suggesting sp^3 bonding in bulk SiC. But for graphitic-like sheet structures, there is charge distribution on the π orbital. Specifically the charge distribution on the π orbital undergoes a change from less than $0.02|e|$ per bond in the initial buckled and unrelaxed graphitic-like structure to about $0.10|e|$ per bond in the final stabilized and flattened graphitic-like sheet structure, leading to an enhancement of the ratio $N_{ij}(\pi)/N_{ij}(\sigma)$ from 0.054 to 0.30 (note that the ratio $N_{ij}(\pi)/N_{ij}(\sigma)$ for graphite is 0.33). The dangling bonds associated with the buckled and unrelaxed graphitic-like sheet structure are eliminated by increasing the charge distribution on the π orbital to form the sp^2 type of bonding. This scenario is reinforced by the examination of the bonding energy ($-E_{ij}$). As shown in Table I, the bonding energy of the relaxed flat graphitic-like structure is about 2.35 eV higher than that of the unrelaxed and buckled sheet structure which is still dominated by the sp^3 -bonding. This then indicates that a transition from the dominant sp^3 bonding in the unrelaxed buckled sheet structure to the sp^2 type of bonding in the relaxed flat sheet structure is energetically feasible. This means, analogous to the case of carbon, different types of bonding are possible between silicon and carbon atoms. Namely, it could be either sp^3 -bonding as in the bulk SiC or sp^2 type of bonding as in the graphitic-like sheet structure. Hence, even though Si atoms ordinarily favor the sp^3 hybridization, the presence of C atoms indeed has a stabilizing effect on the graphitic-like structure of SiC. Our finding that a Si atom and a C atom may combine to form either sp^3 bonding or sp^2 type of bonding in SiC systems holds promise for the formation of other potentially interesting and novel SiC-based structures.

It can also be seen from Table I that a considerable amount of electron charge is transferred from Si site to C site (*i.e.*, $0.31|e|$ for bulk β -SiC and $0.32|e|$ for SiC graphitic-like structure, respectively). Similar magnitudes for charge transfers ($0.45|e|$) between Si and C atoms were reported by other researchers for the case of SiC NT.⁶ This is an indication that the bonding between a Si atom and a C atom in a SiC-based structure also carries a strong ionic bonding flavor.

III. SiC NANOTUBES

Based on our calculation, the cohesive energy per atom of a SiC graphitic-like sheet is 0.49 eV higher than that of the bulk SiC. Therefore, one expects SiC nanotubes formed from such SiC sheets to be metastable structures. A previous theoretical calculation has found weakly buckled structures for SiC NTs when their diameters are less than 1.6 nm.⁶ On the other hand, our calculation shows that an initially buckled graphitic-like SiC sheet stabilizes to a flattened sheet, suggesting that the buckling feature of SiC NTs may depend on their diameters.

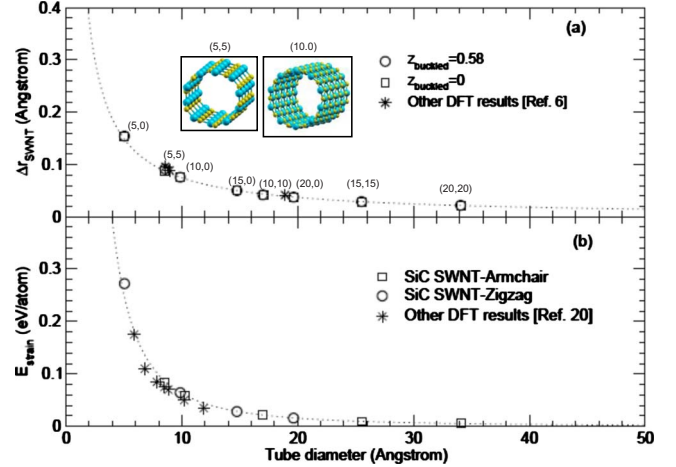


FIG. 2. (Color online) (a) The diameter-dependence of the average radial buckling Δr_{SWNT} (see the text) for both relaxed armchair (m,m) and zigzag ($m,0$) SiC SWNTs, starting from both buckled (squares) and unbuckled initial structures (circles), respectively. The stars are the results from other DFT calculations (Ref. 6). The insets in (a) show the optimized structures corresponding to (5,5) and (10,0) SiC SWNTs (yellow: carbon atoms, blue: Si atoms). (b) The strain energy per atom ($E_{\text{strain}} = E_{\text{tube}} - E_{\text{sheet}}$) as a function of the tube diameter for zigzag (circle) and armchair SiC SWNTs (square) as obtained by our calculation and other DFT studies (Ref. 20) (star).

Buckling is usually associated with the release of the strain energy. It is therefore interesting to examine how the buckling and the corresponding strain energy changes as a function of the diameter of the SiC NT. For these purposes, we performed structural optimization for armchair ($m,0$) and zigzag (m,m) SiC NT structures of increasing diameters (m ranging from 5 to 20) using DFT-based VASP.⁷ The computational scheme used for SiC NTs are the same as those used for SiC graphitic-like sheets. The periodic boundary condition is employed for the quasi-one-dimensional SiC NT structure along the tube axis with a vacuum space (20 Å) between tubes to ensure no interaction between SiC NTs. The plane-wave cutoff is taken as 456 eV with 60 k points for SiC NTs, following the Monkhorst-Pack scheme.¹²

Two kinds of initial configurations of SiC NTs were considered: one is rolled up from a flat graphitic-like sheet, and the other is rolled up from a buckled graphitic-like sheet with a buckling of 0.58 Å. We found that both types of initial configurations led to relaxed structures with similar characteristics as shown in Fig. 2. The Si-C bond length in the relaxed SiC tubes were found to be 1.78 Å, which is similar to the optimized bond length in SiC graphitic sheets and is also in good agreement with other *ab-initio* results.^{6,18–20}

In Fig. 2(a), the degree of radial buckling $\Delta r_{\text{SWNT}} = \bar{r}_{\text{SWNT}}^{\text{C}} - \bar{r}_{\text{SWNT}}^{\text{Si}}$, where $\bar{r}_{\text{SWNT}}^{\text{C}}$ and $\bar{r}_{\text{SWNT}}^{\text{Si}}$ are the average of the radial locations of C and Si atoms, respectively, is shown as a function of the diameter of the tube. While the radial buckling is diameter dependent (*i.e.*, it decreases with increasing tube diameter), it has no dependence on the chirality of the tube. Furthermore, we found that Si atoms move toward the tube axis while C atoms move in the opposite direction, resulting in a slightly buckled structure. Additionally,

a charge transfer of $0.32|e|$ from the Si to the C atoms was found. Similar characteristics were also reported for BN,¹³ GaN,¹⁴ and AlN¹⁵ NTs, where the more electronegative N atoms move outward from the tube axis while group-III atoms (B, Ga, Al) move inward to the tube axis. Since a C atom is more electronegative than the Si atom in the SiC NT (gaining about $0.32|e|$ from the Si atom), it acts like the N atom while the Si atom acts like a group-III atom.

The diameter-dependence of the strain energy per atom $E_{\text{strain}} = E_{\text{tube}} - E_{\text{sheet}}$ of SiC NTs, where E_{tube} and E_{sheet} represent the total energies per atom of the SiC NT and the SiC graphitic sheet, respectively is shown in Fig. 2(b). The strain energy per atom ($d < 1.2$ nm) as obtained by Y. Miyamoto and B. D. Yu²⁰ is also shown in Fig. 2(b). From Figs. 2(a) and 2(b), it can be seen that the buckling as well as the strain energy decrease rapidly with increasing tube diameter and both these quantities approach zero in the limit when the tube diameter goes to infinity, corresponding to a flattened graphitic sheet. This unmistakable correlation between the buckling and the strain energy is an indication that the buckling occurs mainly to release the strain induced by the curvature of the tube. In addition, it is found that the strain energy can be fitted as a function of the tube diameter (d) by the expression $E_{\text{strain}} = E_0 + \alpha/d^2$, where $E_0 = 0$ and $\alpha = 6.3$ (eV Å²). This expression is almost independent of the chirality of the SiC NT, which was also found by Zhao *et al.*⁶ However, the fitting constant E_0 found in Ref. 6 is 0.595 eV. This is because the strain energy in their calculation is defined with respect to the energy of bulk β -SiC, while in the present calculation it is with respect to the energy of SiC graphitic-like sheet.

IV. MULTILAYERED SiC GRAPHITIC-LIKE STRUCTURES

In this section, structural optimizations of multilayered SiC graphitic-like structures have been investigated that will provide the explanation for the occurrence of two different intershell separations (one around ~ 3.8 Å and the other around 4.5 Å) in SiC MWNTs, as reported in experiments.¹ We have performed structural relaxations of multilayered SiC graphitic-like structures using the VASP code⁷ with the number of SiC bilayers ranging from 2 to 4. Two types of bilayer arrangements in the interplanar direction were investigated: (i) the C-C stacking arrangement, and (ii) the Si-C stacking arrangement. Figs. 3(a) and 3(b) illustrate relaxations of two-bilayered SiC graphitic-like structures corresponding to C-C ordering and Si-C ordering, respectively. The structures shown on the left hand columns of Figs. 3(a) and 3(b) correspond to different initial (buckled) configurations with different interlayer spacing values (3.08, 2.31, and 1.54 Å, respectively). The structures shown on the right hand columns of both Figs. 3(a) and 3(b) are the relaxed structures corresponding to those initial structures. After relaxation, all the buckled SiC multilayered structures were stabilized to flattened multilayered structures. The optimized inter-layer spacing was found to be ~ 3.66 Å for the case of Si-C stacking, while it is in the range from 4.47 Å to 4.64 Å for the case of C-C stacking. Structural relaxations performed for three- and four-bilayered SiC graphitic sheets

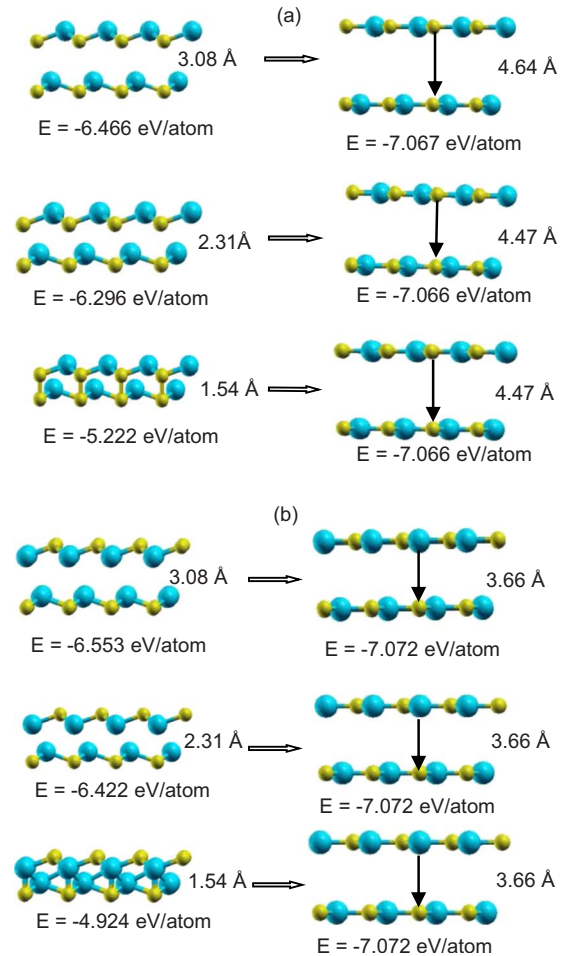


FIG. 3. (Color online) Unrelaxed (left) and relaxed structures (right) of two-bilayered (2BL) SiC graphitic-like structures for two types of interplanar orderings: (a) C-C ordering (top panel) and (b) Si-C ordering (bottom panel), respectively. Silicon and carbon atoms are represented by blue and yellow balls, respectively. Three different initial configurations with the same buckling angle $\theta = \sin^{-1}(z_{\text{buckled}}/b)$ ($b = 1.89$ Å and $z_{\text{buckled}} = 0.63$ Å) but different interlayer spacing values of 3.08, 2.31, and 1.54 Å and their corresponding relaxed structures are shown for both cases (a) and (b). Two energetically close structures ($E = -7.067$ eV/atom and $E = -7.066$ eV/atom) with optimized interlayer spacing values of 4.64 and 4.47 Å were found for the case (a) with C-C ordering. The optimized interlayer spacing for the case (b) with Si-C ordering, was found to be 3.66 Å ($E = -7.072$ eV/atom).

also exhibit two distinct interlayer separations corresponding to Si-C and C-C stacking arrangements.

We have also examined multilayered structures cut from bulk β -SiC along the $\langle 111 \rangle$ direction and those cut from α -SiC along the $\langle 0001 \rangle$ direction. In these cases, we did not find any flattened and well-separated graphitic multilayers after the relaxation. Since only the graphitic-like multilayer structure can stabilize to a structure with interlayer spacing greater than that of a typical bilayer spacing (2.5 Å) in bulk SiC, we conclude that the SiC MWNTs as observed in experiments must have the graphitic-like symmetry and not the cubic symmetry.

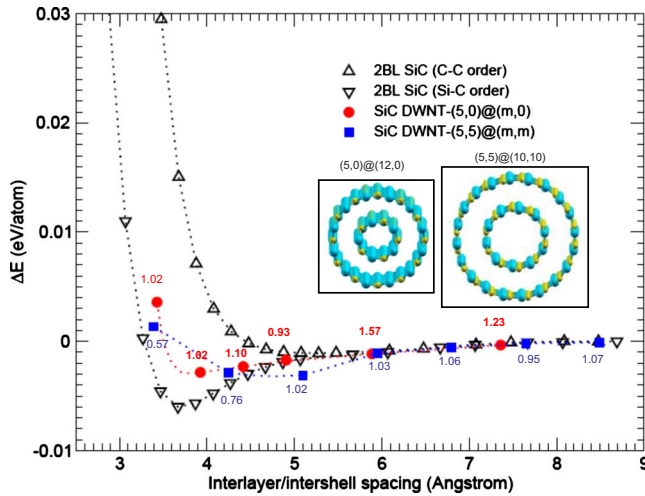


FIG. 4. (Color online) The relative energy per atom corresponding to two-bilayered (2BL) graphitic-like SiC structures ($\Delta E = E_{2BL} - 2E_{sheet}$) (see the text) and SiC DWNTs ($\Delta E = E_{DWNT} - E_{SWNT-1} - E_{SWNT-2}$) (see the text) are shown as a function of the inter-layer spacing and the intershell spacing, respectively for: (i) 2BL SiC with C-C ordering (erect triangles), (ii) Si-C ordering (inverted triangles), (iii) armchair (filled squares) and (iv) zigzag SiC DWNTs (filled circles). The equilibrium interlayer spacing for 2BL SiC graphitic structures occur at 3.67 Å and 4.82 Å, respectively corresponding to Si-C and C-C orderings between the bilayers. The equilibrium intershell separation for the zigzag and that for the armchair SiC DWNTs are found at 3.8 and ~ 4.8 Å, respectively. We have also indicated the value of the quantity α (see the text) for all SiC DWNTs (red: zigzag and blue: armchair) along the ΔE versus intershell distance curves. The insets show the optimized structures corresponding to (5,0)@(12,0) and (5,5)@(10,10) SiC DWNTs, respectively (yellow: carbon atoms, blue: Si atoms).

To understand the equilibrium interlayer distance in multilayered SiC graphitic-like structures, we calculated the relative energy per atom of two-bilayered SiC graphitic sheet ($\Delta E = E_{2BL} - 2E_{sheet}$, where E_{2BL} and E_{sheet} are total energies per atom corresponding to two-bilayers and a flat graphitic sheet, respectively). These results are shown in Fig. 4 for two different types of positional ordering (erect triangles: C-C and inverted triangles: Si-C) between the layers. It can be seen that the equilibrium inter-layer distance is ~ 3.67 Å for Si-C ordering. However, in the case of C-C ordering, the energy curve exhibits an extremely shallow minimum extending from ~ 4.45 to ~ 5.5 Å, with the equilibrium inter-layer spacing at ~ 4.82 Å. This result is consistent with the experimental finding of two different values for the intershell spacing at ~ 3.8 and ~ 4.5 Å in SiC MWNTs.¹ The reason why the equilibrium inter-layer distance depends on the ordering of C and Si atoms in different layers can be explained as follows. In contrast to the carbon-based graphite with no charge redistribution on each site, each C atom gains $0.32|e|$ from each Si atom in the SiC graphitic-like sheet, resulting in long-range electrostatic Coulomb interactions between Si atoms and C atoms not only on the same bilayer but also between atoms in different bilayers. Therefore, in multi-layered SiC graphitic-like structures, in addition to the

weaker van der Waals interactions between SiC layers, there is the competition between the attractive Coulomb interactions and the repulsive Coulomb interactions due to the charge transfer between the Si and the carbon atoms that eventually determines the equilibrium interlayer spacing of the multilayered SiC graphitic-like structure. It is this competition that leads to different ranges of equilibrium inter-layer separations for the case of the Si-C ordering where pairs of Si-C are the nearest inter-layer neighbors as compared to that of the C-C/Si-Si ordering where pairs of C-C/Si-Si are the nearest interlayer neighbors. The energy/atom required to stabilize the multilayered SiC graphitic-like structure is about 1 meV for the C-C ordering and 6 meV for the Si-C ordering, respectively. This means that the dominant effects of the interlayer Si-C attractive interactions over the interlayer C-C/Si-Si repulsive interactions is stronger in the case of Si-C ordering, but weaker in the C-C/Si-Si ordering, leading to a more stable multilayer Si-C graphitic-like structure in the Si-C ordering than that in the C-C ordering.

V. DOUBLE-WALLED SIC NANOTUBES

Obviously, there is no clear one-to-one Si-C or C-C ordering when the SiC graphitic-like multilayers are rolled up to form multiwalled SiC nanotubes. Therefore, the competition between the interlayer C-C/Si-Si and the interlayer Si-C interactions becomes more complex. But it is clear that the intershell spacing of multiwalled SiC nanotubes still depends on the combined effect of repulsive interactions between C (Si) and C (Si) atoms and attractive interactions between C and Si atoms in different shells. To shed light on how this combined effect affects the intershell spacing of SiC MWNTs, we examined the relaxations and the energetics of two sets of commensurate SiC DWNTs, namely, the set of the zigzag nanotubes composed of (5,0)@(m,0) (with $m=12, 13, 14, 15, 17$, and 20) and the set of the armchair nanotubes composed of (5,5)@(m,m) (with $m=9-15$). The relative energy/atom of the relaxed SiC DWNT with respect to corresponding SiC NTs ($\Delta E = E_{DWNT} - E_{SWNT-1} - E_{SWNT-2}$, where E_{DWNT} , E_{SWNT-1} , and E_{SWNT-2} are total energies per atom corresponding to double-wall and the corresponding single-wall tubes, respectively) is shown as a function of the intershell spacing in Fig. 4 for armchair DWNTs (filled squares) and zigzag DWNTs (filled circles). It can be seen that the two curves corresponding to the two sets of SiC DWNTs can be viewed as framed within the borders of the two curves of the two-bilayer graphitic-like structures corresponding to the C-C/Si-Si ordering and Si-C ordering, respectively. The curve for the zigzag DWNTs (5,0)@(m,0) exhibits an energy minimum at ~ 3.8 Å while, for the armchair DWNTs (5,5)@(m,m), the curve exhibits a shallow energy minimum valley extending from 4.2 to 5.1 Å, with the energy minimum at ~ 4.8 Å. These results are consistent with the experimental observations¹ and similar to the cases of multilayered SiC graphitic-like structures.

To shed light on this interesting correlation, we determined the value of the quantity $\alpha = n_{Si-C} / (n_{Si-Si} + n_{C-C})$, which is the ratio of the number of nearest Si-C pairs (n_{Si-C}) to the

total number of the nearest C-C pairs (n_{C-C}) and Si-Si pairs (n_{Si-Si}) for the DWNTs. A ratio greater than one indicates that there are more Si-C pairs (i.e., more attractive interactions) than C-C and Si-Si pairs (i.e., repulsive interactions) combined within the range under consideration while a ratio less than one indicates the opposite. A pair in this study is defined as two atoms located separately at the inner and the outer shells of a SiC DWNT at a certain distance. They are counted within a range that corresponds to the optimized inter-shell separation. The calculated ratio for each DWNT is indicated by the number adjacent to the data representing the particular DWNT in Fig. 4. An examination of these ratios shows that the ratios for the zigzag DWNTs almost exceed one with only one exception (i.e., $\alpha=0.93$ at ~ 4.9 Å) that is removed from the equilibrium inter-shell separation (~ 3.8 Å) while those for the armchair DWNTs in the neighborhood of the equilibrium intershell separation (~ 4.8 Å) are substantially less than one. Thus for the zigzag DWNTs in the neighborhood of the equilibrium intershell separation where the ratios are greater than one, the attractive interaction dominates and yields an equilibrium intershell separation of ~ 3.8 Å while for the armchair DWNTs in the neighborhood of its equilibrium intershell separation where the ratios are less than one, the repulsive interaction dominates and leads to an equilibrium intershell separation of ~ 4.8 Å, consistent with the cases of the multilayered graphitic-like structures discussed above. The result thus suggests that the nature of the intershell neighbors is the key factor determining the equilibrium intershell spacing. While it is computationally not feasible to determine the equilibrium intershell spacing for general SiC MWNTs of any chirality because the structures of their shells are in general incommensurate, it is not unreasonable to suggest, based on the above consideration, that the experimentally observed two ranges of intershell spacing of SiC MWNTs are the consequences of the competition between interlayer attractive and repulsive Coulomb interactions. Specifically, if the intershell pairs are dominated by Si-C pairs, the equilibrium intershell spacing will be in the range of ~ 3.8 Å while if the intershell pairs are by C-C and Si-Si pairs, the intershell spacing will be in the range of ~ 4.8 Å.

We also examined the radial buckling feature of SiC DWNTs and the deviation of the radial buckling in SiC DWNTs ($\Delta r_{DWNT} - \Delta r_{SWNT}$, where Δr_{DWNT} and Δr_{SWNT} are the degrees of the radial buckling of the inner/outer shell of the SiC DWNT and of the corresponding SiC SWNT, respectively) as a function of the intershell spacing. As shown in Fig. 5, when the intershell spacing is less than 5 Å the buckling feature of the inner shell of SiC DWNTs is weakened while that of outer shell is enhanced, compared to the corresponding isolated SiC NT. Such behavior is almost independent of the chirality of SiC DWNTs. This reveals that when two shells are close, the Coulomb interaction between neighboring shells can affect the buckling behavior of the tubes. When the intershell spacing increases, the effect of the Coulomb interaction will be weakened as can be seen from the zero deviation of the radial buckling in SiC DWNT with large intershell spacing shown in Fig. 5.

Finally, we have investigated the electronic band structures of the armchair and the zigzag SiC single/double wall

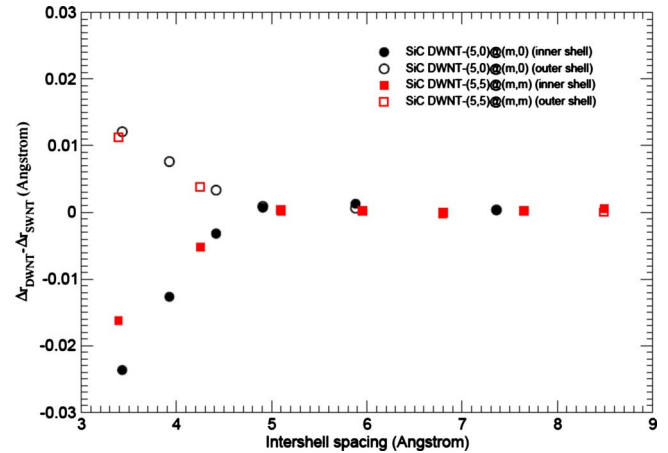


FIG. 5. (Color online) The dependence on the intershell separation of the deviation of the radial buckling in SiC DWNTs $\Delta r_{DWNT} - \Delta r_{SWNT}$ (see the text). The open (filled) squares represent the results of the outer shells (inner shells) for the armchair (5,5)@ (m,m) SiC DWNTs ($m=9-15$). The open (filled) circles represent similar quantities for the zigzag (5,0)@ (m,0) SiC DWNTs ($m=12, 13, 14, 15, 17, \text{ and } 20$).

NTs, as well as the SiC graphitic-like sheet structure. We found that the electronic band structures of zigzag SiC SWNTs exhibit direct band gaps and those of armchair SiC SWNTs exhibit indirect band gaps (see Fig. 6), similar to the results found by other DFT calculations.^{6,20} The electronic band structures of SiC DWNTs, on the other hand, exhibit a combination of the band structures of two SiC SWNTs corresponding to their inner and the outer shells, respectively. Accordingly, the zigzag SiC DWNTs has a direct band gap and the armchair SiC DWNTs has an indirect band gap (Fig. 6).

The corresponding energy gaps are summarized in Fig. 7. For a given diameter of the SiC SWNT, the energy gap of the armchair tubes is larger than that of the zigzag tubes with similar diameters. We also found that the energy gap of the

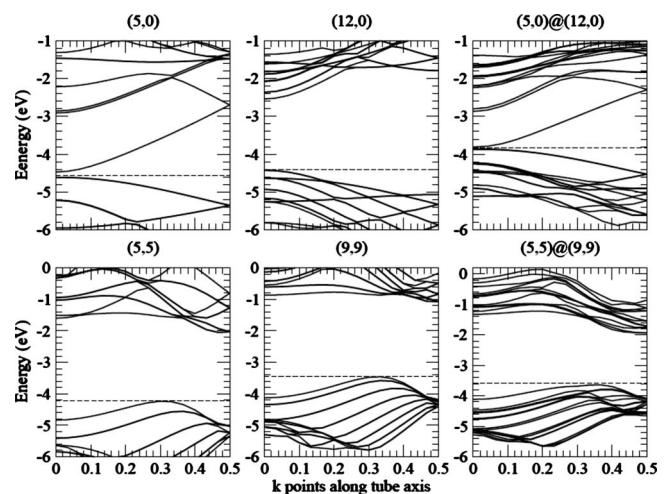


FIG. 6. SiC Band Structures for (5,0)@ (12,0) SiC DWNTs and (5,5)@ (9,9) SiC DWNTs and the band structures for corresponding SiC SWNTs. Fermi energy locations corresponding to each of these cases are also indicated (dashed lines).

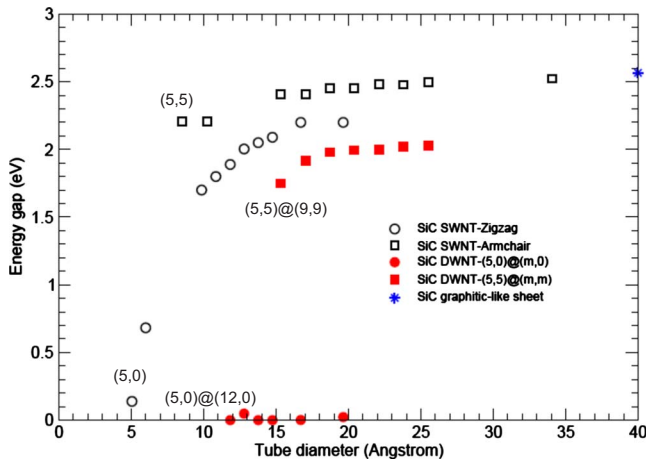


FIG. 7. (Color online) The energy gap as a function of the tube diameter are shown for SiC DWNTs and SiC SWNTs, where the results for armchair DWNTs and SWNTs are depicted by filled and open squares, respectively, while those for zigzag DWNTs and SWNTs are depicted by filled and open circles, respectively. The energy gap of the SiC graphitic-like sheet ~ 2.54 eV is also indicated (star). Chiral indices of selected SiC SWNTs/DWNTs are explicitly indicated to identify their corresponding energy gaps.

SiC SWNT increases with increasing diameter of the tube and almost saturate to the value of the SiC graphitic-like sheet (2.54 eV) when the diameter is larger than 20 Å. For SiC DWNT with its diameter defined by the diameter of its outer shell, we found that the energy gap is basically related to its inner shell. Furthermore, the energy gap of the armchair SiC DWNTs (5,5)@(m,m) is smaller than that of corresponding-isolated inner tube (5,5), and the zigzag SiC DWNTs (5,0)@(m,0) almost show metallic behavior, with energy gap somewhat smaller than the corresponding inner tube (5,0). Such reduction indicates that the Coulomb interaction between the neighboring shells of the SiC DWNTs may not only affect the buckling behavior but also indirectly the electronic structure in the double walled SiC NTs.

VI. CONCLUSION

We have carried out a comprehensive study of the structure, energetics, and the bonding nature of SiC graphitic-like structures and SiC nanotubes based on *ab-initio* simulations.⁷ Our study of SiC graphitic sheets yields two major findings: (1) The bonding nature between a Si atom and a C atom could be, in addition to sp^3 -type as in bulk β -SiC and α -SiC, sp^2 -type as in SiC graphitic-like sheet structures and SiC NTs. The capability of forming sp^3 bond as well as sp^2 bond between a Si atom and a C atom provides the SiC-based systems with the flexibility of forming potentially interesting and novel structures. (2) Because of the charge redistribution between the Si atom and the C atom in SiC graphitic-like multilayer structures and the SiC DWNTs, the interlayer Coulomb interactions are mainly responsible for the equilibrium intershell spacing in SiC MWNTs. Such interactions lead to two ranges of inter-shell spacing as observed in the experiments, depending on whether the dominant nearest inter-shell neighbors are of the Si-C type or the C-C (Si-Si) type. Our study on the energetics of SiC SWNTs has indicated a clear correlation among the strain energy, the degree of buckling in the cylindrical shell, and the charge redistribution between C and Si. Our study on the electronic structures of SiC single/double walled NTs also indicates two issues. (i) SiC SWNTs have semiconductor nature with direct energy gap in zigzag SWNTs and indirect energy gap in armchair SWNTs, respectively. The energy gap increases with increasing diameter of the tube and will saturate to that of SiC graphitic-like sheet. (ii) The energy gap of double walled SiC NTs is mainly dependent on the electronic structure of the inner shell, with some smaller effect from the intershell Coulomb interaction.

ACKNOWLEDGMENT

This work was supported by the Kentucky Science and Engineering Foundation under Grant No. KSEF-753-RDE-007.

- ¹X.-H. Sun, C.-P. Li, W.-K. Wong, N.-B. Wong, C.-S. Lee, S.-T. Lee, and B.-K. Teo, *J. Am. Chem. Soc.* **124**, 14464 (2002).
- ²X. T. Zhou, N. Wang, H. L. Lai, H. Y. Peng, I. Bello, N. B. Wong, C. S. Lee, and S. T. Lee, *Appl. Phys. Lett.* **74**, 3942 (1999); S. Zhu, Hong-An Xi, Qin Li, and Ruoding Wang, *J. Am. Ceram. Soc.* **88**, 2619 (2005).
- ³W. L. Zhou, K. Sun, E. Muñoz, A. B. Dalton, S. Collin, L. M. Wang, A. A. Zakhidov, and R. H. Baughman, *Microsc. Microanal.* **9**, 334 (2003).
- ⁴L. Z. Pei, Y. H. Tang, Y. W. Chen, C. Guo, X. X. Li, Y. Yuan, and Y. Zhang, *J. Appl. Phys.* **99**, 114306 (2006); L. Z. Pei, Y. H. Tang, X. Q. Zhao, Y. W. Chen, and C. Guo, *ibid.* **100**, 046105 (2006).
- ⁵G. L. Harris, *Properties of Silicon Carbide* (INSPEC, Institution of Electrical Engineers, London, 1995).
- ⁶M. Zhao, Y. Xia, F. Li, R. Q. Zhang, and S.-T. Lee, *Phys. Rev. B* **71**, 085312 (2005).

- ⁷G. Kresse and J. Hafner, *Phys. Rev. B* **48**, 13115 (1993); G. Kresse and J. Furthmüller, *ibid.* **54**, 11169 (1996); *Comput. Mater. Sci.* **6**, 15 (1996).
- ⁸D. R. Alfonso, S.-Y. Wu, C. S. Jayanthi, and E. Kaxiras, *Phys. Rev. B* **59**, 7745 (1999).
- ⁹C. Leahy, M. Yu, C. S. Jayanthi, and S. Y. Wu, *Phys. Rev. B* **74**, 155408 (2006); S. Y. Wu, C. S. Jayanthi, C. Leahy, and M. Yu, in *Hand book of Materials Modeling*, edited by S. Yip (Springer, New York, 2005).
- ¹⁰D. Vanderbilt, *Phys. Rev. B* **41**, 7892 (1990); K. Laasonen, R. Car, C. Lee, and D. Vanderbilt, *ibid.* **43**, 6796 (1991); K. Laasonen, A. Pasquarello, R. Car, C. Lee, and D. Vanderbilt, *ibid.* **47**, 10142 (1993).
- ¹¹Y. Wang and J. P. Perdew, *Phys. Rev. B* **44**, 13298 (1991).
- ¹²H. J. Monkhorst and J. D. Pack, *Phys. Rev. B* **13**, 5188 (1976).

- ¹³E. Hernández, C. Goze, P. Bernier, and A. Rubio, *Phys. Rev. Lett.* **80**, 4502 (1998).
- ¹⁴S. M. Lee, Y. H. Lee, Y. G. Hwang, J. Elsner, D. Porezag, and T. Frauenheim, *Phys. Rev. B* **60**, 7788 (1999).
- ¹⁵M. Zhao, Y. Xia, D. Zhang, and L. Mei, *Phys. Rev. B* **68**, 235415 (2003).
- ¹⁶M. Yu, I. Chaudhuri, C. Leahy, S. Y. Wu, and C. S. Jayanthi, *J. Chem. Phys.* **130**, 184708 (2009); Wei Quan Tian, M. Yu, C. Leahy, C. S. Jayanthi, and S. Y. Wu, *J. Comput. Theor. Nanosci.* **6**, 390 (2009).
- ¹⁷M. Yu, S. Y. Wu, and C. S. Jayanthi, *Physica E* **42**, 1 (2009).
- ¹⁸A. Mavrandonakis, G. E. Froudakis, M. Schnell, and M. Muhlhäuser, *Nano Lett.* **3**, 1481 (2003).
- ¹⁹M. Menon, E. Richter, A. Mavrandonakis, G. E. Froudakis, and A. N. Andriotis, *Phys. Rev. B* **69**, 115322 (2004).
- ²⁰Y. Miyamoto and B. D. Yu, *Appl. Phys. Lett.* **80**, 586 (2002).